

Applications of VAS and TOVS to Tropical Cyclones

Christopher S. Velden,¹
William L. Smith,²
and Max Mayfield³

Abstract

Initial results are presented on research designed to evaluate the usefulness of Visible Infrared Spin Scan Radiometer Atmospheric Sounder (VAS) data in tropical cyclone applications. It is part of the National Aeronautics and Space Administration funded VAS demonstration, and the National Oceanic and Atmospheric Administration (NOAA) Operational VAS Assessment (NOVA) program. The University of Wisconsin (UW) Space Science and Engineering Center (SSEC) and the National Environmental Satellite, Data, and Information Service (NESDIS) Development Laboratory at the SSEC have been working with the National Hurricane Center (NHC), and the NOAA/Environmental Research Laboratories Atlantic Oceanographic and Meteorological Laboratory—Hurricane Research Division (HRD) to explore the different uses of geostationary satellite VAS data in tropical cyclone analysis and forecasting. Because of the cloud-penetrating capability of the microwave component of the TIROS Operational Vertical Sounder (TOVS), polar orbiting satellite TOVS soundings in cloudy regions are used in some cases to enhance the VAS products along with cloud drift and water vapor motion winds derived from VAS imagery. This report describes some of the VAS/TOVS products being generated and evaluated on the Man-computer Interactive Data Access System (McIDAS) at the UW-SSEC and the NHC.

1. Introduction

The 1982 and 1983 hurricane seasons served as “test grounds” for McIDAS software (Suomi *et al.*, 1983), display programs, subjective analyses, and editing procedures at the UW-SSEC of VAS data over the North Atlantic Ocean area for use by the NHC in tropical cyclone applications. Initially, several problems were encountered in the processing and displaying phase of the operation. By the end of the 1983 season, however, considerable progress had been made toward providing timely (quasi-real time, within two to five hours of data reception), high-quality analyses and displays of mass, motion, and moisture patterns for NHC evaluation.

The VAS radiometer contains eight visible channel detectors and six thermal detectors that sense infrared radiation in 12 spectral bands. Retrieval of accurate temperature and moisture profiles from these radiances can be accomplished using the radiative transfer equation and solutions which rely on the physical properties of the measurements (Smith, 1983). Associated thicknesses can be derived from these pro-

files, height fields can be built from the thickness fields and a lower (1000 mb) reference field discussed in the next section, and winds can be derived from these height fields (also discussed in the next section). More complete descriptions of the VAS and TOVS instruments, their retrieval algorithms, and operating modes are given by Smith (1983) and Smith *et al.* (1979).

Routine daily VAS coverage for NHC evaluation began in June 1982. Normally, one data set at approximately 1300 GMT was provided to the NHC in near real time. Coverage normally included most of the Geostationary Operational Environmental Satellite (GOES)-East viewing area between 17 to 55°N and 30 to 110°W. To fit in with VISSR operational imaging commitments, the data were obtained in two 10-minute swaths separated by approximately 30 minutes. (Details of the VAS measurement characteristics and mode of operations are summarized by Smith *et al.*, 1981). On specifically-designed hurricane research days, coverage was considerably expanded. Three 10-minute swaths, each about a half hour apart, are combined to cover the tropical disturbance. An example of data coverage on a hurricane research day for Tropical Storm Beryl of 1982 is shown in Fig. 1. The figure shows 6.7 μm (mid tropospheric) water vapor imagery with plotted radiosonde identification numbers (there are a few more stations not shown in the Caribbean Sea area); note the lack of conventional upper air data in this region. Data sets of smaller areal extent centered on a significant tropical disturbance (cover) were processed up to three times a day in quasi-real time to provide the NHC with analyses of the storm environment. The imagery shown (see cover) is constructed from a combination of the VAS 6.7 μm mid tropospheric H₂O emission observations and 11 μm atmospheric window cloud and surface emission observations. Clouds are delineated by white areas, high water vapor concentrations

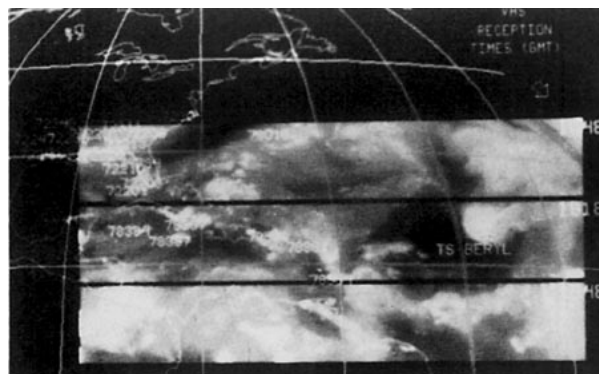


FIG. 1. Example of data coverage on a hurricane research day for Tropical Storm Beryl of 1982. Radiosonde identification numbers are printed over the 6.7 μm water vapor (mid tropospheric) imagery. (VAS HURRICANE SCHEDULE II; 1 SEPTEMBER 1982.)

¹ Space Science and Engineering Center, 1225 West Dayton St., Madison, WI 53706.

² NOAA/NESDIS Development Laboratory, 1225 West Dayton St., Madison, WI 53706.

³ NOAA/NWS Satellite Field Services Station, 1320 South Dixie Highway, 6th Floor, Coral Gables, FL 33146.

by blue and green areas, and dry, cloud-free regions by dark brown and black areas. Also shown is a plot of upper level (approximately 200 mb) winds (in knots) around Hurricane Debby for 0000 GMT on 16 September 1982 from a combined wind data set that will be described in Section 4.

A display program on McIDAS was developed to facilitate a quick look by NHC at selected fields derived from the VAS data. As improvements in retrieval, analysis, and display procedures were developed together with a better understanding of the VAS measurements qualities, including its limitations, the NHC personnel were better able to evaluate the tropical storm analysis and forecasting capabilities of the VAS over oceanic areas for operations. Evaluation efforts to determine optimum use of these data are expected to continue on a near real time basis through the 1984 hurricane season.

2. Comparisons with radiosondes

Comparisons of the VAS temperature and moisture profile retrievals with selected tropical radiosondes (Bermuda, San Juan, and West Palm Beach) were made by the NHC during the 1983 hurricane season (for details of VAS sounding retrieval methods, see Smith, 1983). Temperatures, dewpoints, thicknesses, heights, and winds were evaluated; the results of a combination of all comparisons are summarized in Table 1. Most comparisons were made at 1200 GMT, and wherever the radiosonde and VAS soundings were sufficiently close in time and space (within approximately two hours and approximately 100 km, respectively). Winds that accompany the VAS temperature retrievals are derived from geopotential heights analyzed at constant pressure levels. The height data used to construct the analyses are provided from the VAS

TABLE 1. Differences between VAS and radiosonde derived parameters for Bermuda, San Juan, and West Palm Beach (1 August–30 November 1983).

| Parameter | Mean Difference (D) ^a | Standard Deviation (σ) ^b | Difference Range | Number of Cases (n) |
|------------------------------------------------------------------------|-----------------------------------|----------------------------------------------|--------------------------------------------|---------------------|
| T850 | 1.4°C | 1.2°C | -1.6 to 4.7°C | 70 |
| T700 | 0.2°C | 1.3°C | -2.3 to 3.4°C | 70 |
| T500 | 0.4°C | 1.2°C | -2.4 to 2.7°C | 69 |
| T400 | 1.2°C | 1.5°C | -3.0 to 4.0°C | 66 |
| T300 | 0.9°C | 1.7°C | -3.6 to 4.3°C | 66 |
| T200 | 0.0°C | 1.6°C | -5.5 to 3.4°C | 63 |
| TD850 | 2.7°C | 4.5°C | -5.8 to 21.8°C | 70 |
| TD700 | 4.6°C | 8.3°C | -8.1 to 29.7°C | 70 |
| TD500 | 0.9°C | 9.9°C | -9.0 to 21.9°C | 69 |
| TD400 | 2.8°C | 7.8°C | -9.8 to 23.8°C | 66 |
| TD300 | 4.1°C | 8.1°C | -18.2 to 24.1°C | 66 |
| Z850 | 7 m | 10 m | -23.0 to 31.0 m | 68 |
| Z700 | 13 m | 13 m | -21.0 to 36.0 m | 67 |
| Z500 | 18 m | 19 m | -26.0 to 38.0 m | 67 |
| Z400 | 22 m | 20 m | -37.0 to 66.0 m | 65 |
| Z300 | 30 m | 27 m | -52.0 to 71.0 m | 63 |
| Z200 | 32 m | 37 m | -63.0 to 110.0 m | 62 |
| Z500-850 | 12 m | 15 m | -31.0 to 63.0 m | 69 |
| Z400-850 | 16 m | 18 m | -42.0 to 50.0 m | 67 |
| Z300-850 | 23 m | 26 m | -63.0 to 71.0 m | 65 |
| Z500-700 | 6 m | 12 m | -28.0 to 52.0 m | 68 |
| Z400-700 | 10 m | 16 m | -39.0 to 35.0 m | 66 |
| Z200-400 | 9 m | 28 m | -78.0 to 60.0 m | 63 |
| Z200-850 | 24 m | 41 m | -114.0 to 106.0 m | 63 |
| Magnitude of vector wind difference ($\text{m} \cdot \text{s}^{-1}$) | | | | |
| 850 mb | 4 $\text{m} \cdot \text{s}^{-1}$ | 2 $\text{m} \cdot \text{s}^{-1}$ | 0.0 to 14.0 $\text{m} \cdot \text{s}^{-1}$ | 64 |
| 700 mb | 4 $\text{m} \cdot \text{s}^{-1}$ | 3 $\text{m} \cdot \text{s}^{-1}$ | 0.0 to 11.0 $\text{m} \cdot \text{s}^{-1}$ | 64 |
| 500 mb | 4 $\text{m} \cdot \text{s}^{-1}$ | 2 $\text{m} \cdot \text{s}^{-1}$ | 1.0 to 13.0 $\text{m} \cdot \text{s}^{-1}$ | 61 |
| 400 mb | 5 $\text{m} \cdot \text{s}^{-1}$ | 3 $\text{m} \cdot \text{s}^{-1}$ | 1.0 to 19.0 $\text{m} \cdot \text{s}^{-1}$ | 62 |
| 300 mb | 7 $\text{m} \cdot \text{s}^{-1}$ | 5 $\text{m} \cdot \text{s}^{-1}$ | 1.0 to 27.0 $\text{m} \cdot \text{s}^{-1}$ | 59 |
| 200 mb | 10 $\text{m} \cdot \text{s}^{-1}$ | 7 $\text{m} \cdot \text{s}^{-1}$ | 2.0 to 40.0 $\text{m} \cdot \text{s}^{-1}$ | 54 |

$${}^a D = \frac{1}{n} \sum_{i=1}^{i=n} D_i, \text{ where } D_i = (\text{VAS}_i - \text{RAOB}_i) \text{ for the } i^{\text{th}} \text{ case. } {}^b \sigma = \sqrt{\frac{1}{n} \sum (D_i - D)^2}$$

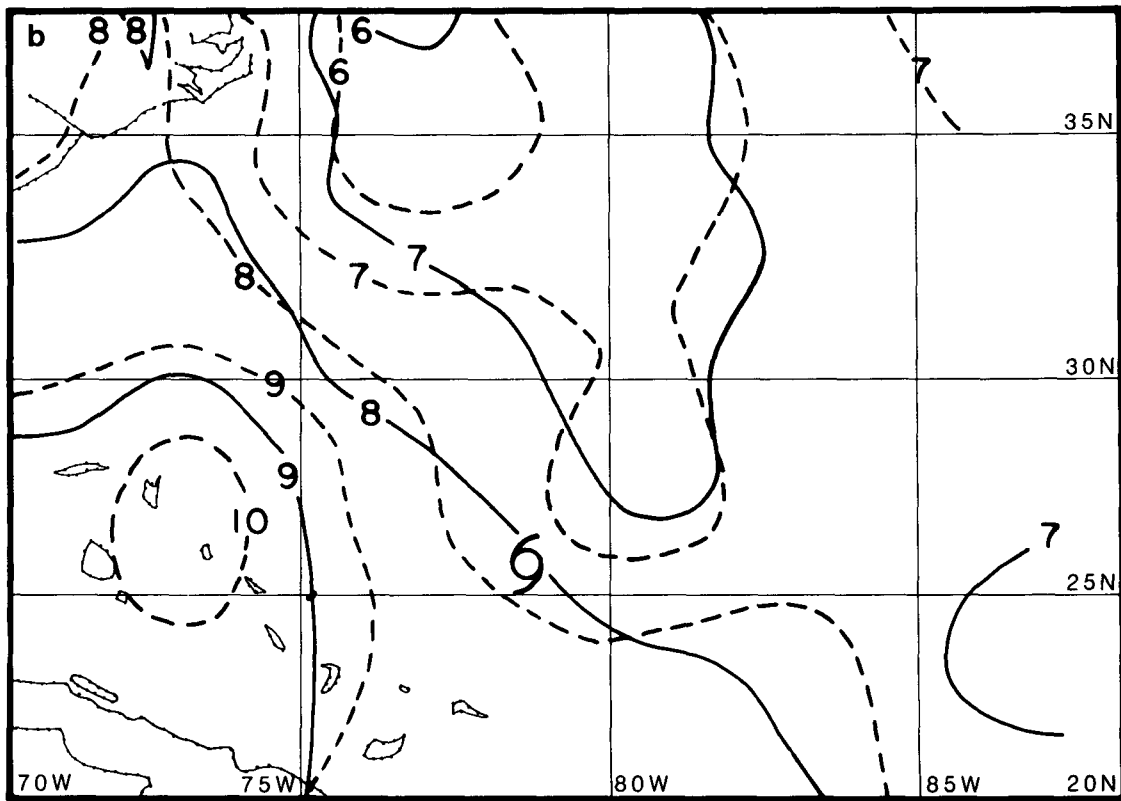
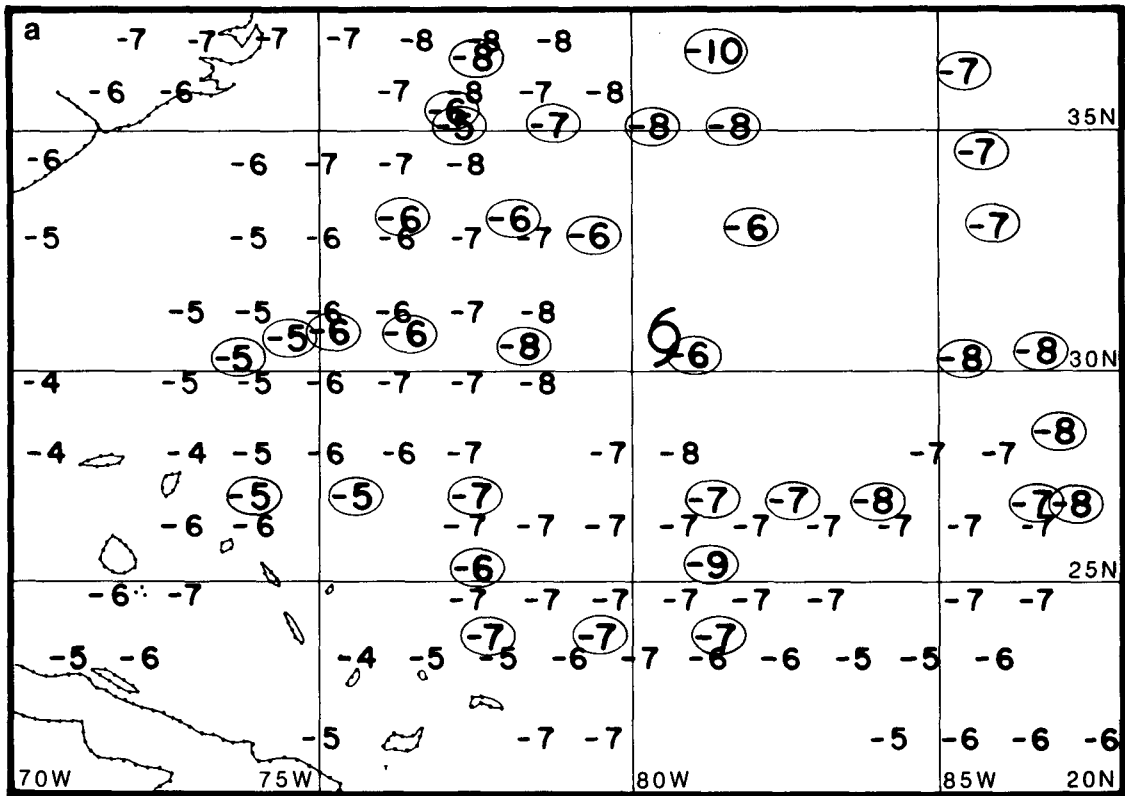


FIG. 2. (a) Comparison of the 500 mb temperatures ($^{\circ}\text{C}$) observed by the ODWs (circled numbers) and VAS near Hurricane Debby for 0000 GMT on 16 September 1982. (b) Comparison of objective analyses of VAS (solid) and ODW (dashed) 700 mb temperature ($^{\circ}\text{C}$) values for Hurricane Debby on 15 September 1982 at 0000 GMT.

temperatures and mixing ratios, and a lower reference level that is a surface height estimated from a topography file and a surface pressure field produced from objective analyses of mean sea level temperature and 1000 mb heights (Hayden, 1983, personal communication; Montgomery, 1984). The latter are based on conventional surface observations and a global forecast field. The curvature term is included in these gradient winds. The VAS gradient winds had a mean directional difference of about 30 degrees (not shown). Several factors may contribute to these differences, such as deficient lower reference 1000 mb height fields due to inadequate conventional surface reports across some oceanic regions. Confidence in the gradient wind accuracy is higher in clear areas where sounding precision and density are the greatest. However, these results suggest that gradient winds computed in this manner are generally less useful than cloud motion winds (when both are available) in the NHC tropical analyses. The VAS temperature observations, however, were considered good. The standard deviations of the difference between the VAS and radiosonde values were on the order of 1 to 1.5 degrees. Associated thicknesses derived from the temperature profiles were excellent when compared with the radiosonde observations. The NHC expressed confidence in the temperature and thickness parameters. As expected, the differences are larger for moisture because the VAS lower vertical resolution moisture profiles cannot capture highly-structured vertical features as well as the radiosonde.

3. Comparisons with dropsondes

A comprehensive meteorological data set, including VAS data, is being constructed from observations of Hurricane Debby from 13–17 September 1982. NOAA Office of Aircraft Operations aircraft flew prescribed tracks throughout the environment of Hurricane Debby on two missions (14–15 September and 15–16 September 1982). During this time, a dropwindsonde experiment was performed by the HRD, providing an opportunity to compare the VAS soundings produced in real time with Omega dropwindsonde (ODW) observations. Fig. 2a shows an example comparison of the 500 mb temperatures at 0000 GMT on 16 September 1982 observed by the ODWs and the VAS (dropsondes circled). Fig. 2b shows a comparison of objective analyses of the VAS and ODW 700 mb temperature values for 0000 GMT on 15 September 1983. As may be seen, the thermal patterns indicated by the independent observations are in close agreement. Fig. 3 illustrates a specific VAS retrieval and ODW comparison on a Stüve diagram. Except for the height of the moist layer, the comparison is quite good. Numerical comparisons, similar to the previously-noted radiosonde comparisons, were made by the NHC and are shown in Table 2. Comparisons were made wherever the ODW and the VAS soundings were sufficiently close in time and space. The results of the comparisons were quite similar to the radiosonde comparisons, with the temperatures and thicknesses having the smallest differences. (No VAS gradient winds were generated in real time for 14–15 September; the comparisons shown are for the 15–16 September case only.)

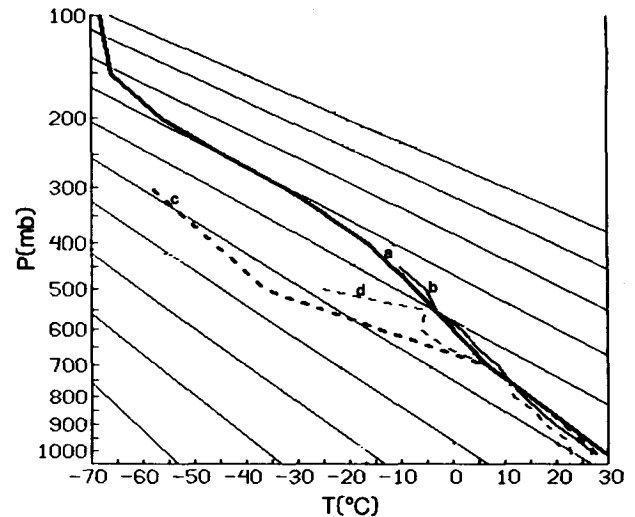


FIG. 3. VAS retrieval/and ODW comparison on Stüve diagram. a) VAS Air Temperature. b) ODW Air Temperature. c) VAS Dew-point Temperature. d) ODW Dew-point Temperature.

4. Circulation from the VAS cloud drift, water vapor motion, and gradient wind observations

Studies have indicated that the deep layer mean wind field around a tropical cyclone is one of the best indicators of the storm's steering current (Chan and Gray, 1982). One of the main goals of the cooperative program is to provide the NHC with an analysis of the satellite-derived deep layer mean wind "steering current" for forecasting hurricane movement. For Tropical Cyclone Debby, three VAS data sets were processed each day (0000, 1200, and 1800 GMT on 13–17 September 1982) covering a large area centered on the hurricane. To further enhance the VAS derived data sets, selected NOAA 6 and NOAA 7 polar orbiting satellite passes over Debby were processed to take advantage of the TOVS microwave profile retrievals and derived gradient winds in the cloudy regions of the hurricane not achievable from the VAS infrared data. These microwave soundings were combined with the VAS soundings into a single data set and manually edited for consistency using the McIDAS. To further enhance the atmospheric circulation information, high and low level cloud drift (Mosher, 1979) and mid-level water vapor motion (Mosher and Stewart, 1981) winds were derived from the VAS imagery and added to the gradient wind data set, with further manual editing of the winds for consistency. The water vapor motion winds were derived from a three-hour loop of the 6.7 μm water vapor imagery which has peak radiance contributions originating from about 400 mb. Radiosondes were used for quality control in the editing process where available. The final wind set consisting of VAS gradient, TOVS gradient (in some cases), cloud drift, and water vapor motion winds for three levels—approximately 850, 400, and 200 mb (see cover)—was used to derive a deep layer (850–200 mb) mean (dlm) wind analysis. These three levels actually represent layers, since the cloud drift and water vapor motion data are not all exactly at the indicated heights (± 50 mb and ± 100 mb, respectively). The small number of TOVS gradient winds

TABLE 2. Differences between VAS and ODW derived parameters for 14–15 and 15–16 September 1982.

| Parameter | Mean Difference (D) ^a | Standard Deviation | Difference Range | Number of Cases (n) |
|---------------------------------------------------------|----------------------------------|-----------------------|-----------------------------|---------------------|
| T850 | 1.4°C | 1.3°C | -1.4 to 4.9°C | 42 |
| T700 | - 0.3°C | 1.2°C | -2.7 to 2.6°C | 42 |
| T500 | - 0.1°C | 1.3°C | -2.4 to 2.3°C | 35 |
| T400 | 0.2°C | 1.4°C | -3.1 to 3.3°C | 24 |
| TD850 | 1.6°C | 3.2°C | -5.0 to 9.8°C | 42 |
| TD700 | 3.6°C | 5.2°C | -8.9 to 14.9°C | 42 |
| TD500 | -12.5°C | 7.0°C | -36.4 to 6.0°C | 35 |
| TD400 | - 8.9°C | 7.6°C | -25.3 to 7.5°C | 24 |
| Z850 | - 6 m | 23 m | -68 to 26 m | 42 |
| Z700 | 0 m | 22 m | -58 to 41 m | 42 |
| Z500 | 1 m | 24 m | -56 to 44 m | 35 |
| Z400 | 2 m | 27 m | -54 to 47 m | 24 |
| Z400–850 | 11 m | 17 m | -16 to 45 m | 24 |
| Z500–850 | 6 m | 14 m | -18 to 43 m | 35 |
| Z400–700 | 4 m | 14 m | -16 to 34 m | 24 |
| location (nm) | 29 nm | 15 nm | 6 to 54 nm | 42 |
| time (min) | 38 min | 29 min | 2 to 108 min | 42 |
| Magnitude of vector wind difference m · s ⁻¹ | | | | |
| 850 mb | 7 m · s ⁻¹ | 4 m · s ⁻¹ | 1 to 14 m · s ⁻¹ | 23 |
| 700 mb | 7 m · s ⁻¹ | 4 m · s ⁻¹ | 1 to 16 m · s ⁻¹ | 23 |
| 500 mb | 5 m · s ⁻¹ | 3 m · s ⁻¹ | 1 to 12 m · s ⁻¹ | 22 |
| 400 mb | 7 m · s ⁻¹ | 4 m · s ⁻¹ | 3 to 16 m · s ⁻¹ | 13 |

$${}^a D = \frac{1}{n} \sum_{i=1}^{i=n} D_i, \text{ where } D_i = (VAS_i - RAOB_i) \text{ for the } i^{\text{th}} \text{ case. } {}^b \sigma = \sqrt{\frac{1}{n} \sum (D_i - D)^2}$$

shown on the cover is due to the fact that these winds are used only in areas void of cloud drift and VAS gradient winds. These areas usually correspond to the storm center and adjacent featureless heavy cloud areas where cloud drift winds are difficult. The cloud-penetrating capabilities of the microwave radiances (after careful editing of precipitation attenuation) make soundings and derived gradient winds possible in these areas. However, due to the relatively poor resolution of the microwave radiances (5 km vertical and 110 km spatial), the TOVS gradient winds are subject to larger errors than the VAS gradient winds and should be used with discretion. Regression equations were derived by Sanders *et al.* (1980) based on tropical radiosonde data for estimating the tropospherically-averaged flow from information at three levels (850, 500, and 250 mb), and a similar set of equations derived for the three levels in this study (850, 400, and 200 mb) were used to produce the dlm analysis (Goldenberg, 1984, personal communication). The entire process from data ingest to the completion of the dlm analysis can be accomplished on the McIDAS in two to two-and-a-half hours.

Combined wind vectors for the three levels over Hurricane Debby's environment for 0000 GMT on 16 September 1982 are shown in Figs. 4a-c. The cyclonic circulation of Debby is present at all three levels, with the strongest winds at low levels, as would be expected. The circulation quickly becomes anticyclonic a way from the center at upper levels with

a large ridge providing an outflow channel to the east of Debby. The amplitude of this ridge was underforecast by the global analysis, with the result that many models forecast the storm to move on a more northeasterly path rather than the more northerly path that the storm followed before turning to the northeast once over the ridge. Debby can be seen embedded in a mid-latitude trough with a closed center at mid and upper levels to the north of the storm.

The combination of high density cloud drift winds in cloudy areas, high density gradient winds derived from VAS retrievals in clear areas, water vapor motion winds at mid levels, and gradient winds derived from TOVS microwave retrievals (when available) provide a much better than normally available description of the wind fields surrounding tropical cyclones in a typically data-sparse region. A Barnes objective map analysis scheme (Barnes, 1973) is used to derive the three individual level streamline analyses from the raw data. The deep layer mean wind analysis is then derived from the three individual level analyses using the regression equations on a 1.0 degree mesh grid. A final step is to remove the tropical cyclone vortex, if one is present, and define the mean wind steering current over the storm. This is first done by determining the position of the storm and its radius of influence. The radius of influence, as determined by the NHC, is the average distance from the storm center to the outermost analyzed closed isobar around the storm. This is com-



FIG. 4. (a) Upper tropospheric (approximately 200 mb) edited combined wind vectors (kts) around Hurricane Debby for 0000 GMT on 16 September 1982. (b) Same as (a) except for mid tropospheric (approximately 400 mb). (c) Same as (a) except for lower tropospheric (approximately 850 mb). The + indicates calm to east of Debby.

pared to the outermost closed streamline in the dlm analysis. Whichever is greater is used; however, they usually are very close in length. The grid values within this radius of influence are then zeroed out. The current storm direction and speed, as determined by the NHC, are inserted into the grid at the storm position. The grid points within the radius of influence

are then given values using bilinear interpolation between the surrounding data and the storm position value. While it is recognized that the determination of current storm direction and speed can be fairly subjective, especially in storms with nondescript centers and no reconnaissance support, this technique was used and will be evaluated in the next section. An example of the final dlm streamline and speed analyses with the vortex removed for Debby on 16 September 1982 is shown in Fig. 5.

Deep layer mean wind analyses are being provided to the AOML-HRD for all the time periods processed around Debby and for all 1983 Atlantic tropical cyclones, in order to make comparisons with conventional atmospheric analyses of the North Atlantic Ocean area and assess the forecast utility of greatly enhanced wind observations over this area, which is virtually void of conventional observations. Testing and numerical comparisons will be done with a modified version (Goldenberg, 1983, personal communication) of the SANBAR (SANDers BARotropic) model (Sanders *et al.*, 1975). In the meantime, a simpler procedure has been tested at the UW-SSEC as described in the following section.

5. Prediction of tropical cyclone motion

As may be seen in Fig. 5 from the locations of Hurricane Debby at 12-hour intervals beginning at 0000 GMT on 16 September 1982, the tropical cyclone follows the satellite-derived deep layer mean wind analysis streamlines (from 0000 GMT on 16 September 1982 data) fairly closely out to 72 hours. Greater deviations from the streamline pattern obviously can be expected at longer durations from the analysis time, since steady state is assumed and the streamline fields in reality are constantly changing and evolving with time. This streamline field, however, serves as a good approximation of the steering current and subsequent short range storm track forecast. With assumptions that the deep layer mean wind steering current theory holds, and that the abundance of wind data in a normally data-sparse region would improve the dlm analysis, a simple trajectory model was developed at the UW-SSEC to test on the Hurricane Debby data. While it

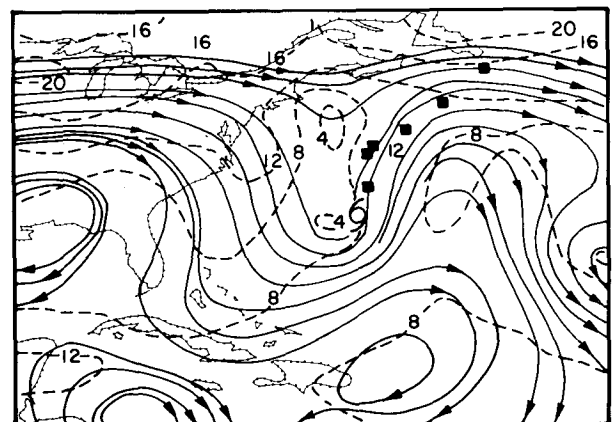


FIG. 5. Final 850–200 mb satellite derived deep layer mean wind streamline (solid) and speed (dashed in m/sec) analysis for Hurricane Debby at 0000 GMT on 16 September 1982. Solid squares indicate Debby's storm track every 12 hours.

is recognized that trajectory forecasting of tropical cyclone movement is not a new concept, the method was employed using the satellite-derived deep layer mean wind analyses to assess the accuracy of the streamline field as an approximate steering current and as an initial analysis for more sophisticated forecast models (Le Marshall *et al.*, 1984). The purpose of this exercise is not so much to devise a hurricane forecast model as to evaluate the impact of the VAS data in combination with the TOVS and cloud drift data in the simplest way possible.

The streamlines are given by the solution to the following equations:

$$\begin{aligned} dx/dt &= u(x,y) \\ dy/dt &= v(x,y). \end{aligned}$$

These equations are solved numerically by using the Adams method (Hildebrand, 1962). This method assumes that $u(x,y)$ and $v(x,y)$ vary linearly between mesh points on the grid analysis and results in the following formulas for the path:

$$\begin{aligned} x_{k+1} &= x_k + hU_k + \frac{h}{2}(U_k - U_{k-1}) \text{ and} \\ y_{k+1} &= y_k + hV_k + \frac{h}{2}(V_k - V_{k-1}), \end{aligned}$$

where (x_k, y_k) and (x_{k-1}, y_{k-1}) are the previous positions of the source point with corresponding velocities (U_k, V_k) and (U_{k-1}, V_{k-1}) , and h is the time step. The velocity components at an arbitrary point in the grid analysis field are found using bilinear interpolation. A typical model run takes only a few seconds on the McIDAS. An example forecast for Hurricane Alicia landfill is shown in Fig. 6.

Comparisons of mean forecast errors (MFE) for several

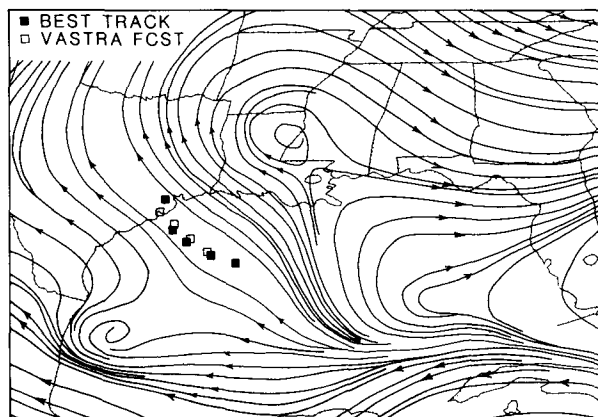


FIG. 6. Final 850-200 mb satellite-derived deep layer mean wind streamline analysis for Hurricane Alicia at 1200 GMT on 16 August 1983. Solid squares indicate Alicia's storm track every 12 hours. Open squares indicate the VASTRA forecast out to 48 hours.

different operational models used by the NHC, the official forecasts, and the VASTRA (VAS TRAjectory) model for selected homogeneous cases when satellite-derived deep layer mean wind data were available from Debby of 1982, and Alicia, Barry and Chantal of 1983, are shown in Table 3. Initial positioning error (Neumann and Pelissier, 1981) was removed from the MFE in all cases. Performance of specified models relative to the CLIPER model is shown in Fig. 7. From Table 3 and Fig. 7, it can be seen that the VASTRA forecasts compare favorably with the official forecasts and the other operational models. While it is recognized that

TABLE 3. Comparisons of MFE (nm) for selected homogeneous cases during Hurricane Debby of 1982 and Hurricanes Alicia, Barry, and Chantal of 1983 (official and MFM forecasts are not issued for 36 and 72 h, respectively).

| Model | 12 | # of cases | Forecast Intervals (h) | | | | 48 | # of cases | 72 | # of cases |
|--------------------|----|------------|------------------------|------------|-----|------------|-----|------------|-----|------------|
| | | | 24 | # of cases | 36 | # of cases | | | | |
| Official Forecasts | 54 | (20) | 126 | (17) | — | — | 289 | (12) | 305 | (9) |
| VASTRA | 53 | (20) | 111 | (17) | — | — | 232 | (12) | 311 | (9) |
| NHC 67 | 52 | (18) | 110 | (15) | 195 | (12) | 269 | (10) | 393 | (8) |
| NHC 72 | 50 | (18) | 114 | (15) | 178 | (12) | 224 | (10) | 530 | (8) |
| CLIPER | 59 | (18) | 137 | (15) | 251 | (12) | 318 | (10) | 430 | (8) |
| VASTRA | 51 | (18) | 104 | (15) | 146 | (12) | 201 | (10) | 375 | (8) |
| HURRAN | 72 | (16) | 171 | (12) | 287 | (10) | 358 | (9) | 356 | (8) |
| VASTRA | 56 | (16) | 115 | (12) | 151 | (10) | 208 | (9) | 297 | (8) |
| NHC 73 | 57 | (15) | 125 | (13) | 155 | (9) | 206 | (8) | 528 | (7) |
| VASTRA | 52 | (15) | 112 | (13) | 164 | (9) | 194 | (8) | 362 | (7) |
| SANBAR | 66 | (16) | 141 | (14) | 269 | (10) | 373 | (9) | 570 | (7) |
| VASTRA | 56 | (16) | 107 | (14) | 167 | (10) | 231 | (9) | 362 | (7) |
| MFM | 54 | (9) | 95 | (7) | 123 | (5) | 191 | (5) | — | — |
| VASTRA | 45 | (9) | 85 | (7) | 134 | (5) | 187 | (5) | — | — |

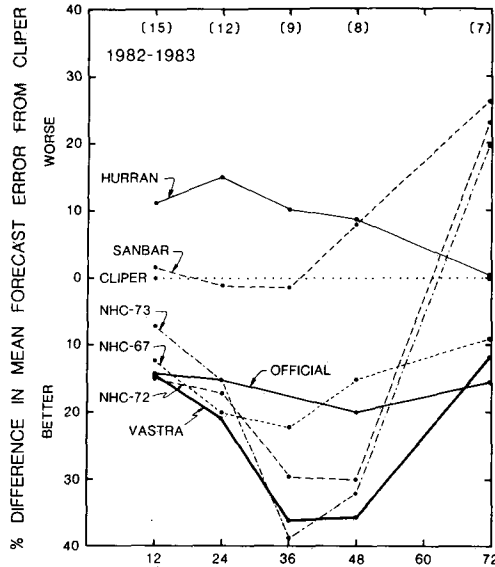


FIG. 7. Performance of specified models relative to the performance of the CLIPER model for 1982 and 1983 cases studied. The sample is homogeneous, with the numbers in parentheses giving sample size. Forecasts are unavailable for any model at 60 hours and for official forecasts at 36 hours.

these data represent a relatively small statistical set, it is believed that the good quality and much-improved density of wind data over the oceanic regions are at least in part responsible for the encouraging results. Several VASTRA forecasts (Debby cases) included in these results were not run in real time. More importantly, however, the data were collected, edited and analyzed for the most part in quasi-real time. VASTRA forecasts from 1983 storms were actually made in real time in a quasi-operational testing mode, and were made available to the NHC. It is the intent of the authors to show what is possible but not yet currently achieved in an operational mode. VASTRA will be tested in an operational atmosphere in the 1984 hurricane season, and only then will an assessment be made on it specifically by NHC personnel.

The model was also run on the same cases without inserting current storm motion (not shown) and using simple bilinear interpolation of the surrounding data within the radius of influence with slightly poorer (5 to 10%) results. However, these case study storms had fairly good reconnaissance flight coverage and steady storm tracks, so that initialized storm motion estimates provided by the NHC were good on the average. It is suggested that the current storm motion be used when there is a high confidence in it by NHC, either because of a clearly defined center and steady motion or continuous reconnaissance flight reports. It should not be used when confidence in the estimate is low due to heavy overcast over the center, lack of reconnaissance data, etc.

6. Intensity from TOVS soundings

Atlantic tropical cyclone intensities were also monitored at the UW-SSEC utilizing the NOAA polar orbiting satellite microwave measurements to provide an estimate of the

strength of the upper tropospheric warm core, which is statistically correlated to the surface central pressure and maximum winds (Kidder *et al.*, 1978; Grody and Shen, 1982; Velden and Smith, 1983). Fig. 8 is an example of the agreement between the surface pressure and maximum sustained wind speed estimates from the TOVS microwave technique, with the NHC official best track data for Tropical Cyclone Barry. Scatter diagrams relating ΔT_{250} with central pressure and maximum winds (as estimated by NHC) are shown in Figs. 9a and b. Included in the statistics shown in Fig. 9, which are an update from previous findings, are comparisons from the 1982 and 1983 hurricane seasons. Experimental use of the TOVS microwave intensity estimates by the NHC to augment existing methods was continued in the 1984 Atlantic hurricane season.

7. Concluding remarks and future work

Future cooperative research using the VAS and TOVS data with the NHC and the AOML-HRD is planned through the 1984 hurricane season. Daily VAS and TOVS data sets were again processed and sent to the NHC in near real time for their evaluation.

An effort is currently underway to use trajectory analyses from consecutive deep layer mean wind analyses in a numerical model. To help generate the initial wind analysis for the barotropic model (SANBAR), the sequence of previous wind

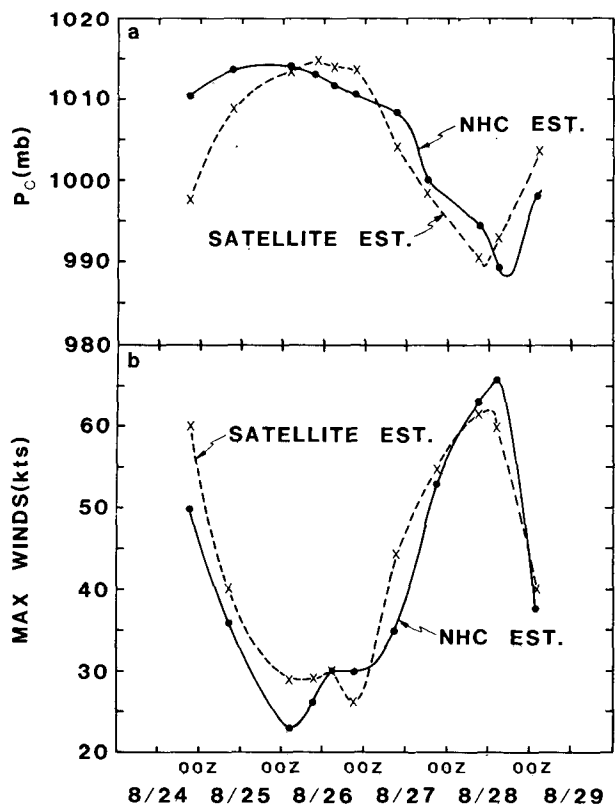


FIG. 8. Comparison of the National Hurricane Center "best track" versus the satellite microwave estimates of (a) central pressure, and (b) maximum winds for Barry.

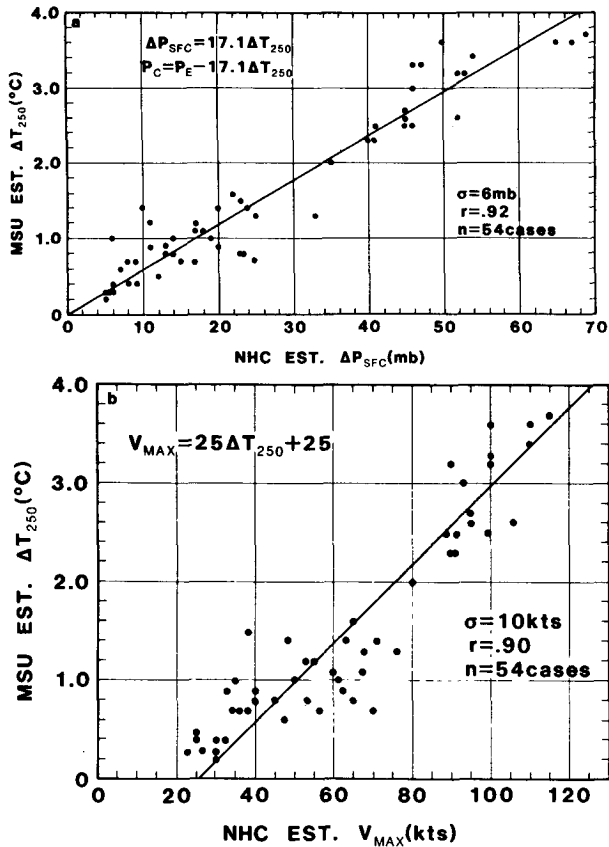


FIG. 9. Comparison of ΔT_{250} versus National Hurricane Center estimated (a) central surface pressure, and (b) maximum winds. P_E is average environmental surface pressure surrounding the storm at a 6° radius, n is number of cases in the sample, r is correlation coefficient, and σ is standard deviation.

analyses will be used to augment the field at the initial time ($t = 0$); in effect, an extrapolation of the analyses to $t = 0$ in order to fill in the satellite data-void areas. These ideas have been used successfully on the VAS geopotential data in conjunction with quasi-geostrophic models (Lewis *et al.*, 1983). In the context of hurricane tracking, the barotropic constraint of absolute vorticity conservation will be used to couple the wind fields in time.

Continued research into hurricane track forecasting using the satellite-derived deep layer mean wind analyses in the SANBAR model and the complete VAS/TOVS sounding and wind data sets in primitive equation forecast models is planned as part of the NOAA Operational VAS Assessment (NOVA) program.

Acknowledgments. The authors wish to thank the personnel of UW-SSEC, NESDIS/DL, NHC, and AOML-HRD who contributed to the research reported here. Special thanks are extended to Professor Verner E. Suomi for his enthusiastic support and guidance, Dr. Robert Burpee of HRD for providing the dropsonde data, Drs. Robert Fox and Paul Menzel for providing the McIDAS/VAS facility support necessary for the application reported here, Stan Goldenberg, Robert E. Kohler, Dr. John Lewis, Gary Wade, Dr. Christopher Hayden, Tod Stewart, and Dr. Arthur Pike for their contributions to the software and data processing aspects of this project, and to Mrs. Gail Turluck for the handling of the manuscript. The continued enthusiastic support of Dr. R. Sheets of the NHC is responsible for much of the rapid progress toward defining the tropical storm applications of VAS. This research was supported by NASA Grant #NAS5-21965.

References

Barnes, S. L., 1973: Mesoscale objective analysis using weighted time series observations. NOAA Technical Memorandum ERL NSSL-62, National Severe Storms Laboratory, 1313 Halley Circle, Norman, Okla., 60 pp.

Chan, J. C. L., and W. M. Gray, 1982: Tropical cyclone movement and surrounding flow relationships. *Mon. Wea. Rev.*, **110**, 1354-1374.

Goldenberg, S., 1983: Personal communication. NOAA/ERL Atlantic Oceanographic and Meteorological Laboratories, Hurricane Research Division, 4301 Rickenbacker Causeway, Miami, Fla.

—, 1984: Personal communication. NOAA/ERL Atlantic Oceanographic and Meteorological Laboratories, Hurricane Research Division, 4301 Rickenbacker Causeway, Miami, Fla.

Grody, N. and W. C. Shen, 1982: Observations of Hurricane David (1979) using the microwave sounding unit. NOAA Technical Report NESL 88, National Oceanic and Atmospheric Administration, National Earth Satellite Service, Washington, D.C., 52 pp.

Hayden, C. M., 1983: Personal communication. NOAA/NESDIS Development Laboratory, 1225 West Dayton Street, 2nd Floor, Madison, Wisc. 53706.

Hildebrand, F. B., 1962: *Advanced Calculus for Applications*. Prentice-Hall, Inc., Englewood Cliffs, N.J., 646 pp.

Kidder, S. Q., W. M. Gray, and T. H. Vonder Haar, 1978: Estimating tropical cyclone central pressure and outer winds from satellite microwave sounder data. *Mon. Wea. Rev.*, **108**, 1458-1464.

Le Marshall, J. F., W. L. Smith, and G. M. Callan, 1984: Hurricane Debby—an illustration of the complimentary nature of VAS soundings and cloud and water vapor motion winds. Submitted to the *Bulletin of the American Meteorological Society*.

Lewis, J. M., C. M. Hayden, and A. J. Schreiner, 1983: Adjustment of VAS and RAOB geopotential analysis using quasi-geostrophic constraints. *Mon. Wea. Rev.*, **111**, 2058-2067.

Montgomery, H., 1984: VAS demonstration description, summary and final report. NASA Publication forthcoming in 1984.

Mosher, F. R., 1979: Cloud drift winds from geostationary satellites. *Atmos. Tech.*, **10**, 53-60.

—, and T. R. Stewart, 1981: Characteristics of water vapor tracked winds. *NAVENVPREDRSCHFAC Contractor Report, CR 81-06*, 51 pp.

Neumann, C. J., and J. M. Pelissier, 1981: Models for the prediction of tropical cyclone motion over the North Atlantic: an operational evaluation. *Mon. Wea. Rev.*, **109**, 522-538.

Sanders, F., A. C. Pike, and J. P. Gaertner, 1975: A barotropic model for operational prediction of tracks of tropical storms. *J. Appl. Meteor.*, **14**, 265-280.

—, A. L. Adams, N. J. B. Gorden, and W. D. Jensen, 1980: Further development of a barotropic operational model for predicting paths of tropical storms. *Mon. Wea. Rev.*, **108**, 642-654.

Smith, W. L., 1983: The retrieval of atmospheric profiles from VAS geostationary radiance observations. *J. Atmos. Sci.*, **40**, 2025-2035.

—, H. M. Woolf, C. M. Hayden, D. Q. Wark, and L. M. McMillin, 1979: The TIROS-N operational vertical sounder. *Bull. Amer. Meteor. Soc.*, **60**, 1177-1187.

—, V. E. Suomi, W. P. Menzel, H. M. Woolf, L. A. Sromovsky, H. E. Revercomb, C. M. Hayden, D. N. Erickson, and F. R. Mosher, 1981: First sounding results from VAS-D. *Bull. Amer. Meteor. Soc.*, **62**, 232-236.

Suomi, V. E., R. Fox, S. S. Limaye, and W. L. Smith, 1983: McIDAS III: A modern interactive data access and analysis system. *J. Climate Appl. Meteor.*, **22**, 766-778.

Velden, C. S., and W. L. Smith, 1983: Monitoring tropical cyclone evolution with NOAA satellite microwave observations. *J. Climate Appl. Meteor.*, **22**, 714-724.